

JAAS

Accepted Manuscript



This is an *Accepted Manuscript*, which has been through the Royal Society of Chemistry peer review process and has been accepted for publication.

Accepted Manuscripts are published online shortly after acceptance, before technical editing, formatting and proof reading. Using this free service, authors can make their results available to the community, in citable form, before we publish the edited article. We will replace this *Accepted Manuscript* with the edited and formatted *Advance Article* as soon as it is available.

You can find more information about *Accepted Manuscripts* in the [Information for Authors](#).

Please note that technical editing may introduce minor changes to the text and/or graphics, which may alter content. The journal's standard [Terms & Conditions](#) and the [Ethical guidelines](#) still apply. In no event shall the Royal Society of Chemistry be held responsible for any errors or omissions in this *Accepted Manuscript* or any consequences arising from the use of any information it contains.

Atomic emission spectrometry in liquid electrode plasma using hourglass microchannel

*Yoshinobu Kohara,^{*a} Yasushi Terui,^b Megumi Ichikawa,^b Kazuko Yamamoto,^c Toshihiro Shirasaki,^c
Kimiyooshi Kohda,^c Tamotsu Yamamoto,^d and Yuzuru Takamura^e*

^a Hitachi Ltd., Central Research Laboratory, 1-280 Higashi-koigakubo, Kokubunji, Tokyo 185-8601,
Japan

^b Hitachi High-Technologies Corporation, 882 Ichige, Hitachinaka, Ibaraki 312-8504, Japan

^c Hitachi High-Tech Science Corporation, 1040 Ichige, Hitachinaka, Ibaraki 312-0033, Japan

^d Micro Emission Ltd., Ishikawa Create Lab, 2-13 Asahidai, Nomi, Ishikawa 923-1211, Japan

^e School of Material Science, Japan Advanced Institute of Science and Technology, 1-1 Asahi-dai,
Nomi, Ishikawa 923-1292, Japan

CORRESPONDING AUTHOR FOOTNOTE

E-mail: yoshinobu.kohara.ud@hitachi.com

Tel: +81-42-323-1111

Abstract

Liquid electrode plasma atomic emission spectrometry (LEP-AES) is a new elemental analysis method that uses microplasma. LEP forms in a vapor bubble generated inside a narrow-center microchannel by using high-voltage DC pulse power. In this study, we used a novel hourglass microchannel having a 3-dimensionally and axisymmetrically narrowed shape, which caused a bright emission roughly 200 times that of the flat microchannel used in our previous study. We observed the spatial distribution of atomic emission and determined the limit of detection (LoD) by utilizing the confirmed spatial distribution. We found that the spatial distribution of atomic emission for 41 elements in our experiments could be classified into three patterns in accordance with maximum emission point: anode side, narrow-center, and cathode side. Atomic emission was measured at the maximum emission point and the calibration curve for each element was made to determine LoD. The LoD of 25 tested elements in our experimental ranged from 1 $\mu\text{g/L}$ for Li to 306 $\mu\text{g/L}$ for V.

Introduction

Elemental analysis is a fundamental component of analytical chemistry and is used for a variety of applications. In the analysis of liquid samples, reliable methods such as atomic absorption spectrometry (AAS), inductively coupled plasma atomic emission spectrometry (ICP-AES), and inductively coupled plasma mass spectrometry (ICP-MS) are widely used, and many studies have been conducted. However, the need for a gas increases the analytical cost, and the complex instruments require frequent maintenance, which makes these methods difficult to apply in the field and in real-time analysis.

One method that overcomes these issues is the use of microplasma sources especially for liquid sample analysis¹⁻⁵. There are a miniaturized atmospheric-pressure thermal plasma jet source⁶, electrolyte-cathode discharge (ELCAD), which is an atmospheric glow discharge in the air gap between a flow-through electrolyte solution cathode and a metal anode⁷⁻¹², liquid-sampling atmospheric-pressure

1 glow discharge (LS-APGD) uses a conductive tube to deliver the sample¹³⁻¹⁴ and so on. The other
2 reported method using both electrodes consisting of solutions is discharge on boiling in a channel¹⁵⁻¹⁷.
3 Also, nanoscale corona discharge in liquids for optical emission spectrometry is reported¹⁸.
4
5
6

7
8 Liquid electrode plasma atomic emission spectroscopy (LEP-AES) was first presented by Takamura's
9 group¹⁹. The working principle of LEP-AES is as follows. A liquid sample with electrolytes is filled
10 inside a microchannel having a narrow center and then high-voltage DC pulse power is applied with
11 electrodes on both sides of the microchannel. As a bubble generated by Joule heating at the
12 narrow-center part expands, the bubble-liquid interfaces work as liquid electrodes for discharge inside
13 the bubble. Compared to conventional ICP-AES, LEP-AES uses very small plasma without gas,
14 resulting in lower analytical cost, less maintenance, and smaller instrument size, which makes it easy to
15 be applied in the field and in real-time analysis.
16
17
18
19
20
21
22
23
24
25
26

27
28 Several studies using LEP-APS have been conducted²⁰⁻³⁰. In these works, microchannels made of
29 Polydimethylsiloxane, resin, and silica were used, and with salts or nitric acid as typical solutions, 800
30 to 2500 V was applied for the emission. In our previous work³¹, we studied the characteristics of LEP in
31 flat microchannels, using Pb, and obtained LoD as low as the $\mu\text{g/L}$ order.
32
33
34
35
36
37

38 In the present study, we used a novel hourglass microchannel having a 3-dimensionally and
39 axisymmetrically narrowed shape, which caused a much brighter emission compared with our previous
40 work. We observed the spatial distribution of atomic emission for 41 elements, and found that the
41 emission profiles could be classified into three patterns. We also determined a detection limit of 25
42 elements in our experimental, which ranged from the $\mu\text{g/L}$ to hundreds $\mu\text{g/L}$ order.
43
44
45
46
47
48
49
50
51
52
53

54 **Experimental**

55 **Instrumentation and experimental conditions**

1 The instrumentation we used is shown in Fig. 1. The hourglass microchannel (Fig. 1A) was made by
2 drilling a square fused silica capillary. The length of the microchannel was 9 mm and the diameter of
3 the main channel was 1.6 mm. The narrow-center was 0.6 mm long and 50 μm wide. Both ends were
4 connected with TeflonTM connectors equipped with Pt electrodes ($\phi 0.5$ mm) and tubing.
5
6
7
8
9

10 Schematic diagrams of the instruments are shown in Fig. 1B and C. In both, the hourglass
11 microchannel is connected to the DC power supply, syringe pump, and optical measurement system
12 described in our previous study³¹. For experiments investigating voltage and pulse width dependence in
13 LEP, the instruments illustrated in Fig. 1B were used. A fiber bundle was set just below the
14 microchannel and the other end was connected to a spectrograph with an intensified CCD camera, as
15 described in our previous study³¹. For spatial distribution observation and derivation of LoD, the
16 instruments shown in Fig. 1C were used. The emission image was focused by achromatic lens (No.
17 47-613, UV to NIR corrected triplet lens, $f = 45$ mm, Edmund, USA) to the slit plane of a spectrograph
18 (SP-2558, Acton Research, USA). A cooled CCD camera (PIXUS-256E, Roper Scientific, USA) was
19 used as the detector of the spectrograph. The microchannel was vertically set with the cathode upside
20 and the solutions were set to flow vertically upward in the microchannel. For the spatial distribution
21 observation, the slit width of the spectrograph was set as wide as 3 mm, and for the sensitivity
22 investigation, the slit width was set to 50 μm . For the LoD estimation, only the data from best location
23 were used. As the microchannel and the slit of the spectrograph aligned, we could select the emission
24 light only from the best location by just assigning the corresponding pixels on CCD camera. The LoD
25 for each element was estimated using $\text{LoD} = 3 \sigma/m$, where σ is the standard deviation of the blank
26 solution measurement data and m is the slope of the calibration curve.
27
28
29
30
31
32
33
34
35
36
37
38
39
40
41
42
43
44
45
46
47
48
49
50

51 The sample solution used in the spatial distribution studies basically consisted of 100 mg/L of each
52 element in 0.1 N nitric acid, with exceptions detailed in the Results and discussion section. Solutions for
53 calibration curve experiments were prepared by diluting the solution with 0.1 N nitric acid. Standard
54
55
56
57
58
59
60

1 solutions were all purchased from Kanto Chemical, Japan. Conditions for each experiment are given in
2
3 the Results and discussion section.
4
5
6
7

8 **Results and discussion**

9 10 **Spatial distribution of atomic emission in LEP using an hourglass microchannel**

11
12
13
14 In our previous study³¹, we used a flat 80- μm depth narrow-center microchannel, but the atomic
15
16 emission was not strong enough for a detailed spatial distribution analysis. To increase the net intensity
17
18 of the emission, in this work we used a novel hourglass microchannel having a 3-dimensionally and
19
20 axisymmetrically narrowed shape (Fig. 1A). We investigated the effect of voltage and pulse width to the
21
22 emission intensity of Pb (405.7 nm), shown in electric supplementary Fig. E1. Compared to the typical
23
24 emission intensity value of Pb in our previous study (flat microchannel, 2.5kV-0.8msec), the emission
25
26 intensity increased by about 200 times (hourglass microchannel, 1.6kV-20msec).
27
28
29
30

31
32 We observed the spatial distribution of atomic emissions in LEP by using a spectrograph with a CCD
33
34 camera. We chose an atomic emission relatively large and well-separated from other emissions so that
35
36 we could clearly obtain a focused image of atomic emission at a wide-opened slit plane without a
37
38 bandpass interference filter. Contrary to our simple preliminary prediction that the atomic emission
39
40 mainly occurs at the narrow center of the microchannel, where the electric field is greatly focused, the
41
42 maximum emission point differed between elements.
43
44
45

46
47 We found that the atomic emission in LEP can be classified into three typical spatial-distribution
48
49 patterns, shown in Fig 2. Before each measurement, an image of the microchannel that had been
50
51 illuminated only for this purpose by a light source was observed using zero order light (Fig. 2A). It is
52
53 clearly shown that narrow center was set in the middle of the image. The three typical patterns had
54
55 maximum emission intensity at the anode side of the narrow center, at the narrow center itself, and at
56
57 the cathode side of the narrow center. Pb was a typical element having anode side emission (Fig. 2B).
58
59
60

1 This emission corresponded to the axis of the conical part at the anode side. Cd was a typical element
2 having its maximum emission at the narrow center (Fig. 2C). K was a typical element having cathode
3 side emission (Fig. 2D). This emission corresponded to the conical part at the cathode side. Emission
4 profiles of cathode side emission were slightly different to the anode side ones in that they emit all over
5 the conical part, and not just around its axis.
6
7
8
9
10

11
12 The spatial distributions and the maximum intensity of atomic emission in LEP in 41 elements were
13 observed and mapped with colors to the periodic table, as shown in Fig. 3A and 3B, respectively.
14
15 Experimental conditions were the same as those in Fig. 2. A large and distinguishable emission wave
16 length was selected for each element and all classification was confirmed with electrode inversion
17 experiments. For the spatial distribution shown in Fig 3A, alkali metals and Co, Ni, and B emitted at the
18 anode side. Neighbor elements, Ga, In, Tl, and Pb, and also Sr, Ba, Fe, and Ag, emitted at the cathode
19 side. The rest of the elements emitted at the narrow center. The reason for this distribution was not yet
20 explained. At the very least, for the purpose of achieving more sensitive detection of the elements in
21 LEP-AES, this knowledge is a key in terms of setting the proper viewpoint for the measurements.
22
23
24
25
26
27
28
29
30
31
32
33

34
35 The same data were mapped with colors depending on the maximum intensity to the periodic table
36 Fig. 3B. The maximum intensity ranged from 125 to 410,000, which were about three logs. The basic
37 trend of the emission was similar to that revealed by other atomic emission spectrometry such as
38 ICP-AES. The emission of alkali metals and alkali earth metals was relatively large. The emission of
39 transition metals was relatively small, especially for refractory metals such as V, Nb, Mo, and W.
40 However, group 11 elements had relatively large emission intensity. Also, metals from groups 12–14
41 had relatively large emission intensity, while the rest of the metalloids and nonmetals emitted weakly.
42
43
44
45
46
47
48
49
50
51

52 A comparison of Figs. 3A and 3B shows that, with some exceptions, the metal elements emitting at
53 the cathode and anode sides tend to have a relatively larger emission and that the metal elements having
54 weak emission tend to have a narrow-center emission. This correlation can be explained by the fact that
55 the emission requiring lower excitation energy can emit at relatively weak electrical field regions while
56
57
58
59
60

1 the one requiring higher exciting energy can emit only in the strong electrical field, which is at the
2 narrow center.
3
4
5
6
7

8 **Calibration curve and detection limit in LEP**

9

10 We determined the best viewpoint for each element for elemental analysis by studying the spatial
11 distribution. As an example, the calibration curve of Pb is shown in electric supplement Fig. E2. A
12 linear dynamics range of at least three logs was shown and LoD was estimated as 3 $\mu\text{g/L}$, which is
13 better than our previous study³², 4 $\mu\text{g/L}$. The cause of the only small increase in sensitivity is not well
14 examined yet, but the fluctuation of background emission could be the one. In total, calibration curves
15 of 25 elements were made and LoD in our experimental was estimated, as shown in Fig. 4. LoD of
16 tested elements in our experimental ranged from 1 $\mu\text{g/L}$ for Li to 306 $\mu\text{g/L}$ for V, which is similar to the
17 results of the flame atomic absorption spectrometry.
18
19
20
21
22
23
24
25
26
27
28
29
30
31
32

33 **Conclusion**

34

35 We applied a new hourglass microchannel in LEP-AES to increase the emission intensity and stability
36 and studied the spatial distribution of atomic emission. We found that emission profiles can be classified
37 into three patterns that can then be used to set the best viewpoint for each element in an LoD experiment.
38 LoD in our experimental ranged from the $\mu\text{g/L}$ to hundreds $\mu\text{g/L}$ order, which is as good as that of
39 flame atomic absorption spectrometry. With observed sensitivity and a simple configuration requiring
40 neither gas nor light sources, LEP-AES is promising for in-field elemental analysis and real-time
41 elements monitoring in a flow-through manner.
42
43
44
45
46
47
48
49
50
51
52
53
54
55

56 **REFERENCES**

57
58
59

- 1 J.A.C. Broekarert, *Anal. Bioanal. Chem.*, 2002, **374**, 182
- 60

- 1
2
3
4
5
6
7
8
9
10
11
12
13
14
15
16
17
18
19
20
21
22
23
24
25
26
27
28
29
30
31
32
33
34
35
36
37
38
39
40
41
42
43
44
45
46
47
48
49
50
51
52
53
54
55
56
57
58
59
60
- 2 J. Franzke, K. Kunze, M. Miclea, K. Niemax, *J. Anal. At. Spectrom.*, 2003, **18**, 802
- 3 V. Karanassios, *Spectrochim. Acta Part B*, 2004, **59**, 909
- 4 J. Franzke, M. Miclea, *Appl. Spectrosc.*, 2006, **60**, 80A
- 5 M. Miclea, and J. Franzke, *Plasma Chem. Plasma Process.*, 2007, **27**, 205.
- 6 T. Ichiki, T. Koidesawa, and Y. Horiike, *Plasma Sources Sci. Technol.*, 2003, **12**, 16
- 7 T. Cserfalvi and P. Mezei, *J. Anal. At. Spectrom.*, 1994, **9**, 345.
- 8 T. Cserfalvi and P. Mezei, *J. Anal. At. Spectrom.*, 2003, **18**, 596.
- 9 P. Mezei and T. Cserfalvi, *Appl. Spectro. Rev.*, 2007, **42**, 573.
- 10 M. R. Webb, F. J. Andrade, and G. Hieftje, *Anal. Chem.*, 2007, **79**, 7899.
- 11 G. Jenkins and A. Manz, *J. Micromech. Microeng.*, 2002, **12**, N19.
- 12 G. Jenkins, J. Franzke, and A. Manz, *Lab. Chip*, 2005, **5**, 711.
- 13 R. K. Marcus and W. C. Davis, *Anal. Chem.*, 2001, **73**, 2903.
- 14 W. C. Davis and R. K. Marcus, *J. Anal. At. Spectrom.*, 2007, **42**, 573.
- 15 B. K. Zuev, V. V. Yagov, M. L. Getsina, and B. A. J. Rudenko, *J. Anal. Chem.*, 2002, **57**, 907.
- 16 B. K. Zuev, V. V. Yagov, and A. S. Grachev, *J. Anal. Chem.*, 2006, **61**, 1172.
- 17 J. Wu, J. Yub, J. Lib, J. Wanga and Y. Ying, *Spectrochim. Acta, Part B*, 2007, **62**, 1269.
- 18 D. Staack, A. Fridman, A. Gutsol, Y. Gogotsi, and G. Friedman, *Angew. Chem. Int. Edn.*, 2008,
34 **47**, 8020
- 19 A. Iiduka, Y. Morita, E. Tamiya, and Y. Takamura, *proc. μ TAS 2004*, 2004, 423.
- 20 H. Matsumoto, A. Iiduka, T. Yamamoto, E. Tamiya, and Y. Takamura, *proc. μ TAS 2005*,
39 2005, 427.
- 21 I. Kumagai, H. Matsumoto, T. Yamamoto, E. Tamiya, and Y. Takamura, *proc. μ TAS 2006*,
43 2006, 497.
- 22 M. Banno, E. Tamiya, and Y. Takamura, *Analytica Chimica Acta*, 2009, **634**, 153.
- 23 K. Nakayama, T. Yamamoto, N. Hata, S. Taguchi, and Y. Takamura, *Bunseki Kagau (in
48 Japanese)*, 2011, **60**, 515.
- 24 S. Kagaya, S. Nakada, Y. Inoue, W. Kamichatani, H. Yanai, M. Saito, T. Yamamoto, Y.
51 Takamura, and K. Tohda, *Analytical Sciences*, 2010, **26**, 515.
- 25 T. Yamamoto, I. Kurotani, A. Yamashita, J. Kawai, and S. Imai, *Bunseki Kagau (in Japanese)*,
54 2010, **59**, 1125.
- 26 M. Kumai and Y. Takamura, *Jpn. J. Appl. Phys.*, 2011, **50**, 096001-1.
- 27 A. Kitano, A. Iiduka, T. Yamamoto, Y. Ukita, E. Tamiya, and Y. Takamura, *Anal. Chem.*,
59 2011, **83**, 9424.

- 1 28 N. H. Tung, M. Chikae, Y. Ukita, P. H. Viet, and Y. Takamura, *Anal. Chem.*, 2012, **84**, 1210.
- 2 29 D. V. Khoai, A. Kitano, T. Yamamoto, Y. Ukita, and Y. Takamura, *Microelectron. Eng.*, 2013,
- 3 **111**, 343.
- 4
- 5 30 D. V. Khoai, T. Yamamoto, Y. Ukita, and Y. Takamura, *Jpn. J. Appl. Phys.*, 2014, **53**, 05FS01.
- 6
- 7 31 Y. Kohara, Y. Terui, M. Ichikawa, T. Shirasaki, K. Yamamoto, T. Yamamoto, and Y.
- 8 Takamura, *J. Anal. At. Spectrom.*, 2012, **27**, 1457.
- 9
- 10
- 11
- 12
- 13
- 14
- 15
- 16
- 17
- 18
- 19
- 20
- 21
- 22
- 23
- 24
- 25
- 26
- 27
- 28
- 29
- 30
- 31
- 32
- 33
- 34
- 35
- 36
- 37
- 38
- 39
- 40
- 41
- 42
- 43
- 44
- 45
- 46
- 47
- 48
- 49
- 50
- 51
- 52
- 53
- 54
- 55
- 56
- 57
- 58
- 59
- 60

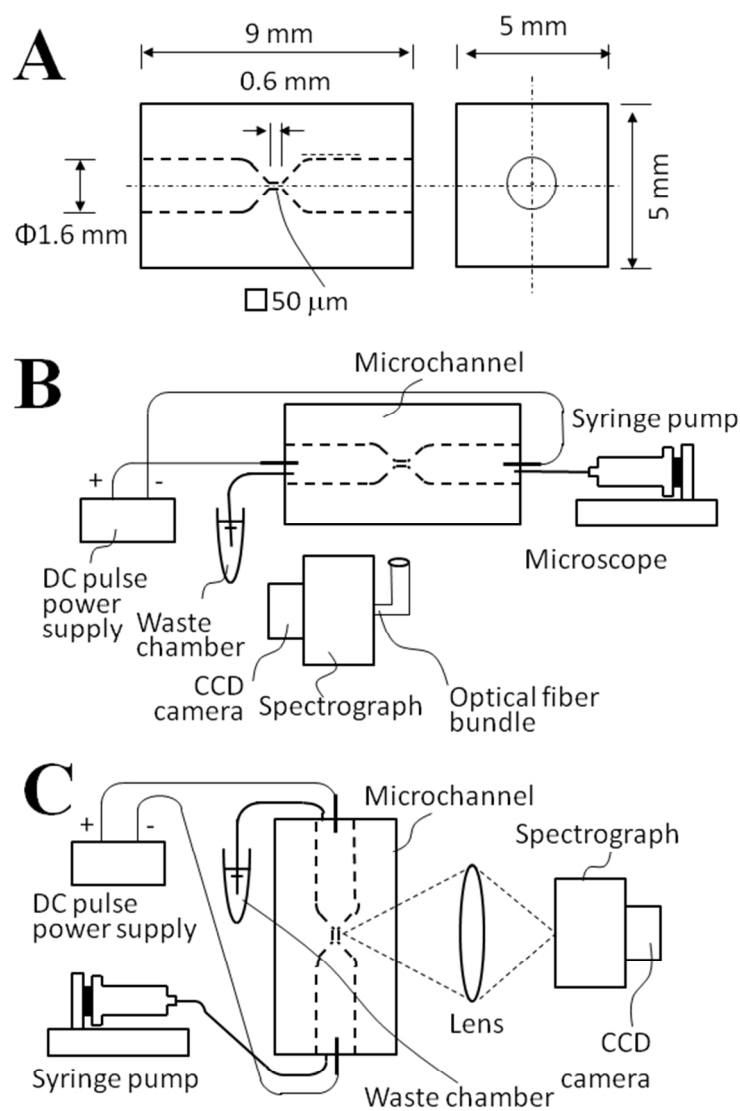


Figure 1. Instrumentations for LEP experiment. (A) Hourglass microchannel. (B) Schematic diagrams of instruments for voltage and pulse width experiment and bubble observation. (C) Schematic diagrams of instruments for spatial distribution observation and derivation of limit of detection.
190x254mm (96 x 96 DPI)

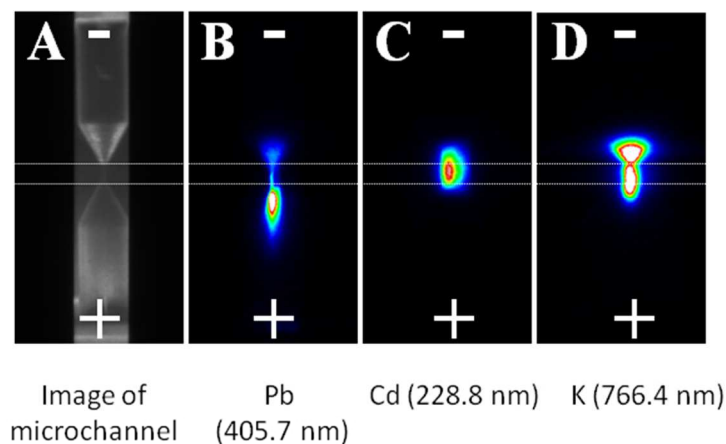


Figure 2. Three patterns of spatial distribution of atomic emission in LEP. (A) Image of microchannel obtained under zero light. (B) Pb (405.7 nm): Typical example of anode side emission. (C) Cd (228.8 nm): Typical example of narrow-centered emission. (D) K (766.4 nm): Example of cathode side emission. All images are flipped vertically from real position because of the lens configuration. Concentration of each element was 100 mg/L and solution was 0.1 N acetic acid. The electrical condition was 2.0kV-20msec. Emission images were all accumulated through 20 pulses.
190x254mm (96 x 96 DPI)

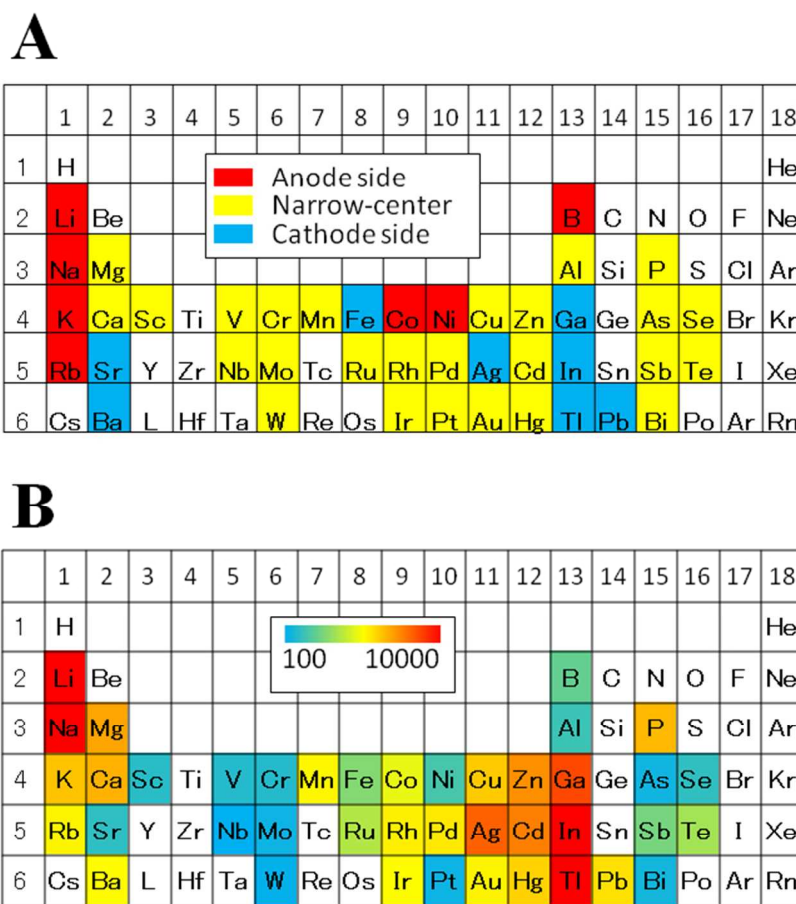


Figure 3. Atomic emission in LEP for 41 elements. (A) Spatial distribution: Red: anode side. Yellow: narrow-center. Blue: cathode side. (B) Maximum intensity values: Colors indicate the intensity, where >10000: Red and <100: Blue. Middle intensities are shown in log gradation. Concentration of each element was 100 mg/L, excluding the elements written below, and solution was 0.1 N acetic acid. The electrical condition was 2.0kV-20msec. Emission images were all accumulated through 20 pulses. Large and distinguishable emission wave lengths were chosen as follows: Li(670.7 nm), B(249.7 nm), Na(588.9 nm), Mg(279.5 nm), Al(396.1 nm, 500 mg/L), P(253.2 nm), K(766.4 nm), Ca(422.6 nm), Sc(391.1 nm), V(437.9 nm, 250 mg/L), Cr(357.8 nm, 1000 mg/L), Mn(257.5 nm), Fe(248.3 nm), Co(241.1 nm), Ni(232.5 nm, 1000 mg/L), Cu(324.7 nm), Zn(213.8 nm), Ga(417.2 nm, 500 mg/L), As(228.8 nm, 1000 mg/L), Se(203.9 nm), Rb(780.0 nm), Sr(496.2 nm, 1000 mg/L), Nb(405.8 nm), Mo(277.7 nm, 500 mg/L), Ru(373.0 nm, 10 mg/L), Rh(343.4 nm, 1 mg/L), Pd(340.4 nm), Ag(328.0 nm), Cd(228.8 nm), In(451.1 nm, 500 mg/L), Sb(259.8 nm), Te(214.2 nm), Ba(455.4 nm, 1000 mg/L), W(400.1 nm), Ir(212.7 nm, 10 mg/L), Pt(249.0 nm), Au(267.5 nm), Hg(253.9 nm, 1 mg/L), Tl(377.5 nm), Pb(405.7 nm), Bi(223.0 nm, 200 mg/L).

190x254mm (96 x 96 DPI)

1
2
3
4
5
6
7
8
9
10
11
12
13
14
15
16
17
18
19
20
21
22
23
24
25
26
27
28
29
30
31
32
33
34
35
36
37
38
39
40
41
42
43
44
45
46
47
48
49
50
51
52
53
54
55
56
57
58
59
60

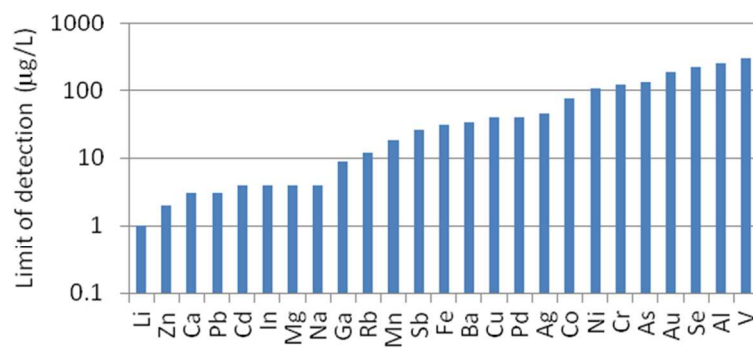


Figure 4. Limit of detection (LoD) in LEP for 25 elements. A calibration curve was made for each element and LoD was estimated. The electrical condition was 1.6kV-20msec. Emission intensity was accumulated for 200 pulses. N = 3 for each concentration.
190x254mm (96 x 96 DPI)